Journal of Engg. Research **Vol. 5 No. (4) December 2017 pp.** *225-235*

المحاكاة العددية للتقدم الاحتراق على محركات الوقود المزدوج مع نماذج الاضطراب مختلفة

هونغليانغ يو*، **، شولين دوان وبيتينغ صن****

* الملاحة والبحرية كلية الهندسة المعمارية، جامعة داليان المحيط، داليان 116023، الصين

** كلية الهندسة البحرية، جامعة داليان البحرية، 1 لينغاي الطريق. داليان، 116026، الصين

الخـلاصـة

من أجل الحصول على نموذج الاضطراب أكثر دقة، تم اعتماد ثلاثة نماذج اضطراب لمحاكاة تقدم الاحتراق على محركات الوقود المزدوج. وبالمقارنة مع البيانات التجريبية، تم التحقق من دقة كل نموذج لمحاكاة تقدم الاحتراق على محركات الوقود المزدوج. ويتم بيان أن متوسط الضغط في الاسطوانة محسوبة لكل نموذج يختلف. ويكون ضغط الذروة في الاسطوانة هو الأكبر من خلال استخدام نموذج (PANS) وهو متوافق أفضل مع البيانات التجريبية، هناك فقط 0.93 ٪ أصغر من البيانات التجريبية. وحساب انبعاثات أسيد النتروجين (NOx) يكون أثر دقة باستخدام نموذج (k-ε). وبالمقارنة مع البيانات التجريبية، فإن الانحراف الحسابي لانبعاثات(O_2) وثاني أكسيد الكربون (CO_2) باستخدام ثلاثة نماذج اضطراب لا يتجاوز 2 ٪. إن حساب نموذج (K-ζ-f) لانبعاثات أول أكسيد الكربون (CO) هو في توافق أفضل مع البيانات التجريبية عندما يكون المحرك في حمولة منخفضة. ومع ذلك، عندما يكون المحرك في حمولة عالية، فإن حساب انبعاث (CO) بواسطة نموذج (PANS) يكون في توافق أفضل مع البيانات التجريبية.

Numerical simulation of combustion progress on dual fuel engines with different turbulence models

Hongliang Yu*,**, Shulin Duan** and Peiting Sun**

Navigation and Naval Architecture College, Dalian Ocean University, 52 Heishijiao Street of Shahekou District, Dalian 116023, China Marine Engineering College, Dalian Maritime University, 1 Linghai Road,. Dalian, 116026, China*

Corresponding Author: yuhongliang19852@163.com

ABSTRACT

In order to get a more accurate turbulence model, three turbulence models had been adopted to simulate combustion progress on dual fuel (DF) engines. Compared with the experimental data, the precision of each model to simulate combustion progress on DF engines was investigated. It is shown that the mean pressure in the cylinder computed by each model is different. The peak pressure in the cylinder is the largest, by using PANS model, and has better agreement with the experimental data, with only 0.93% being smaller than the experimental data. The calculation of NOx emission is more accurate by using k-ε model. Compared with the experimental data, the calculation deviation of O2 and CO2 emission by using three turbulence models does not exceed 2%. The k-ζ-f model calculation of CO emission is in better agreement with the experimental data when the engine is in low load. However, when the engine is in high load, the PANS model calculation of CO emission is in better agreement with the experimental data.

Keywords: DF engine; turbulence models; combustion progress; numerical simulation.

INTRODUCTION

The current design of dual fuel (DF) engines is driven by the need for increased power-densities, improved fuel-efficiencies (Brynolf *et al.,* 2014; Abagnale *et al.,* 2014), reduced emissions (Mohand *et al.,* 2014; Sumit *et al.,* 2014), and lower maintenance cost. Computational techniques have the potential to provide valuable information for the design of DF engines. Over recent years, remarkable progress has been made in the development of computer technology and computational combustion science (Zhou *et al.,* 2015; Henning *et al.,* 2015). In particular, combustion simulation technology has been demonstrated to provide considerably improved predictions of combustion progress (José *et al.,* 2015; Debabrata *et al.,* 2014). The turbulent model, as a basic combustion simulation tool, has been a widespread concern; the correct choice of turbulent model has a great influence on the combustion results (Binbin *et al.,* 2014; Chongmin *et al.,* 2015; Han *et al.,* 2014). So far, regarding research and development of different turbulent models, the general trend is to find a more reasonable method of calculation. However, there is lack of turbulent models that can simultaneously satisfy the reasonableness and accuracy of engineering applications (Yuri *et al.,* 2015; Yee *et al.,* 2015).

Many scholars compared different turbulent models in numerical simulation of engine combustion chambers. Liu Chongyang and Dai Bin (2014) analyzed turbulence models of Standard k-ε, Renormalization group (RNG) k-ε, Realizable k-ε, and Reynolds stress model (RSM) and

conducted a comparison where they found the velocity field calculation results by using Standard k-ε model and Realizable k-ε model were more accurate than those of the RNG k-ε and RSM. Ai Yanting et al. (2015) used the k-ε model, shear stress transport (SST) model, scale adaptive simulation (SAS) model, and large eddy simulation (LES) turbulence model to simulate combustion progress and have shown that the simulation results by using the SST model are in better agreement with the experimental data. Jin Ge et al. (2008) used non-premixed probability density function (PDF) combustion model to compare the Standard k-ε model, RNG k-ε model, and Realizable k-ε model in FLUENT software and found that the Realizable k-ε model is more suitable for the combustion chamber numerical calculation. Leiyong Jiang (2012) used small laminar flame model with 2D a single tube chamber in the FLUENT software and conducted a comparative study with Standard k-ε model, RNG k-ε model, Realizable k-ε model, Standard k-ω model, SST model, and RSM and showed that the RSM turbulence model is superior to other turbulence models. Mongia (2008) mentioned that Giridharan on DACRS mixer flow field calculation shows that the predictions of Realizable k-ε model have the best agreement with the experimental results compared to the Standard k-ε model, RNG k-ε model, and the RSM model in FLUENT.

Thus, the turbulence models used currently in numerical combustion progress simulation are not uniform; many comparative analyses of the results are inconsistent and did not form a unified reference standard. The researchers in their calculations often select different Turbulence models. In this paper, three different turbulence models were used to calculate and analyze the combustion progress of a low-speed marine DF engine in AVL-FIRE software. Therefore, the effect of difference turbulence models were predicted on the combustion pressure and emission products of DF engine, and provided reference for engineering application of turbulence model in the combustion simulation of a low-speed marine DF engine.

TURBULENCE MODEL

The *k-ε* model, PANS model, and *k-ζ-f* model were used to calculate in this work. The three models described in detail follow.

The *k-ε* model

The *k-ε* model is the most widely used turbulence model, particularly for industrial computations, and has been implemented in most CFD codes. It is numerically robust and has been tested in a broad variety of flows including heat transfer, combustion, free surface, and two-phase flows. Despite numerous shortcomings, which have been discovered over the past three decades of use and validation, it is generally accepted that the *k-ε* model usually yields reasonably realistic predictions of major mean-flow features in most situations (Yu *et al.,* 2015). It is particularly recommended for a quick preliminary estimation of the flow field, or in situations where modeling other physical phenomena, such as chemical reactions, combustion, radiation, and multi-phase interactions, bring in uncertainties that outweigh those inherent in the *k-ε* turbulence model. The *k-ε* model consists of two transport equations for *k* and for *ε* (Gan *et al.,* 2014; Yu *et al.,* 2016). The complete standard, *k-ε* model is

$$\rho\frac{\partial k}{\partial t}+\rho U_j\frac{\partial k}{\partial x_j}=P+G-\varepsilon+\frac{\partial}{\partial x_j}\left(\mu+\frac{\mu_t}{\sigma_k}\frac{\partial k}{\partial x_j}\right) \tag{1}$$

$$\rho\frac{D\varepsilon}{Dt}=\left(C_{\varepsilon 1}P+C_{\varepsilon 3}G+C_{\varepsilon 4}k\frac{\partial U_k}{\partial x_k}-C_{\varepsilon 2}\varepsilon\right)+\frac{\partial}{\partial x_j}\left(\frac{\mu_t}{\sigma_\varepsilon}\frac{\partial\varepsilon}{\partial x_j}\right) \tag{2}$$

where $C_{\varepsilon 1}$, $C_{\varepsilon 2}$, $C_{\varepsilon 3}$ and $C_{\varepsilon 4}$ are constant ($C_{\varepsilon 1}$=1.44, $C_{\varepsilon 2}$=1.92, $C_{\varepsilon 3}$=0.8, and $C_{\varepsilon 4}$=-0.373), U is the velocity component (m/s), k is the turbulent kinetic energy (m2/s2), ε is the turbulent kinetic energy dissipation rate (m^2/s^3), x_j is the coordinate components, μ is a kinetic viscosity coefficient (Pa·s), σk and $\sigma\varepsilon$ are the turbulent Prandtl numbers of turbulent kinetic energy and turbulent energy dissipation rate, P is turbulent kinetic energy produced by velocity gradient (m^2/s^2), and G is the turbulent kinetic energy generated by buoyancy (m^2/s^2) .

The PANS model

The PANS model is a recently proposed method by Girimaji (2006). PANS model changes seamlessly from Reynolds-Averaged Navier-Stokes (RANS) to the direct numerical solution of the Navier-Stokes equations (DNS) as the unresolved-to-total ratios of kinetic energy and dissipation varied. The parameter that determines the unresolved-to-total kinetic energy ratio is defined based on the grid spacing, and it is dynamically adjusted at each point at the end of every time step. The basis of this new approach is given next.

The Partially Averaged Navier-Stokes (PANS) equations are written in terms of partially averaged or filtered velocity and pressure fields; thus,

$$\frac{\partial U_i}{\partial t}+U_j\frac{\partial U_i}{\partial x_j}+\frac{\partial\tau(V_i,V_j)}{\partial x_j}=-\frac{1}{\rho}\frac{\partial p}{\partial x_j}+\frac{\partial^2 U_i}{\partial x_i\partial x_j} \tag{3}$$

where the velocity field is decomposed into two components, the partially filtered component and the sub-filter component as

$$V_i=U_i+u_i \tag{4}$$

The closure for the sub-filter stress can be obtained by using the Boussinesq approximation as

$$\tau(V_i,V_j)=-2\nu_u S_{ij}+\frac{2}{3}k_u\delta_{ij} \tag{5}$$

where the eddy-viscosity of unresolved scales is equal to

$$\nu_u=c_\mu\frac{{k_u}^2}{\varepsilon_u} \tag{6}$$

and the resolved stress tensor is given as

$$S_{ij}=\frac{1}{2}\left(\frac{\partial U_i}{\partial x_j}+\frac{\partial U_j}{\partial x_i}\right) \tag{7}$$

The model equations for the unresolved kinetic energy k_u and the unresolved dissipation ε_u are required to close the system of equation given above; thus,

$$\frac{Dk_u}{Dt}=\left(P_u-\varepsilon_u\right)+\frac{\partial}{\partial x_j}\left[\left(\nu+\frac{\nu_u}{\sigma_{ku}}\right)\frac{\partial k_u}{\partial x_j}\right] \tag{8}$$

$$\frac{D\varepsilon_u}{Dt}=C_{\varepsilon 1}P_u\frac{\varepsilon_u}{k_u}-C^*_{\varepsilon 2}\frac{{\varepsilon_u}^2}{k_u}+\frac{\partial}{\partial x_j}\left[\left(\nu+\frac{\nu_u}{\sigma_{\varepsilon u}}\right)\frac{\partial\varepsilon_u}{\partial x_j}\right] \tag{9}$$

The model coefficients are

$$C^*_{\varepsilon 2} = C_{\varepsilon 1} + \frac{f_k}{f_\varepsilon}(C_{\varepsilon 2} - C_{\varepsilon 1}); \sigma_{k,\varepsilon u} = \sigma_{k,\varepsilon}\frac{f_k^2}{f_\varepsilon} \tag{10}$$

where the unresolved-to-total ratios of kinetic energy and dissipation are written, respectively, as

$$f_k = \frac{k_u}{k}, \quad f_\varepsilon = \frac{\varepsilon_u}{\varepsilon} \tag{11}$$

The parameter that determines the unresolved-to-total kinetic energy ratio f_k is defined based on the grid spacing as follows; thus,

$$f_k = \frac{1}{\sqrt{c_u}}\left(\frac{\Delta}{\Lambda}\right)^{2/3} \tag{12}$$

where Δ is the grid cell dimension and Λ is the Taylor scale of turbulence. The PANS asymptotic behavior goes smoothly from RANS to DNS with decreasing f_k. The parameter f_k is implemented in the computational procedure as a dynamic parameter, changing at each point at the end of every time step, and then it is used as a fixed value at the same location during the next time step (Girimaji *et al.,* 2006).

The *k*-ζ-*f* model

This model has been recently developed by Hanjalic, Popovac, and Hadziabdic. They proposed a version of eddy-viscosity model based on Durbin's elliptic relaxation concept (Basara *et al.,* 2010). The aim is to improve the numerical stability of the original $\overline{v^2} - f$ model by solving a transport equation for the velocity scale ratio $\zeta = \overline{v^2}/k$ instead of velocity scale $\overline{v^2}$. The full model is given below:

The eddy-viscosity is obtained from

$$v_t = C_\mu \xi \frac{k^2}{\varepsilon} \tag{13}$$

and the rest of variables are obtained from the following set of model equations; thus,

$$\rho\frac{Dk}{Dt} = \rho(P_K - \varepsilon) + \frac{\partial}{\partial x_j}\left[\left(\mu + \frac{\mu_t}{\sigma_k}\right)\frac{\partial k}{\partial x_j}\right] \tag{14}$$

$$\rho\frac{D\varepsilon}{Dt} = \rho\frac{C^*_{\varepsilon 1}P_k - C_{\varepsilon 2}\varepsilon}{T} + \frac{\partial}{\partial x_j}\left[\left(\mu + \frac{\mu_t}{\sigma_k}\right)\frac{\partial \varepsilon}{\partial x_j}\right] \tag{15}$$

$$\rho\frac{D\zeta}{Dt} = \rho f - \rho\frac{\zeta}{k}P_k + \frac{\partial}{\partial x_j}\left[\left(\mu + \frac{\mu_t}{\sigma_\zeta}\right)\frac{\partial \zeta}{\partial x_j}\right] \tag{16}$$

where the following form of the f equations is adopted from

$$f - L^2\frac{\partial^2 f}{\partial x_j^{\,2}} = \left(C_1 + C_2\frac{P_k}{\zeta}\right)\frac{(2/3 - \zeta)}{T} \tag{17}$$

and the turbulent time scale T and length scale L are given by

$$T = \max\left(\min\left(\frac{k}{\varepsilon}, \frac{a}{\sqrt{6}C^V_\mu |S|\zeta}\right), C_T\left(\frac{\nu^3}{\varepsilon}\right)^{1/2}\right) \tag{18}$$

$$L = C_L \max\left(\min\left(\frac{k^{3/2}}{\varepsilon}\right), C_\eta \frac{\nu^{3/4}}{\varepsilon^{1/4}}\right) \tag{19}$$

Additional modifications to the ε equation are that the constant $C_{\varepsilon 1}$ is dampened close to the wall; thus,

$$C^*_{\varepsilon 1} = C_{\varepsilon 1}\left(1 + 0.045\sqrt{1/\zeta}\right) \tag{20}$$

This is computationally more robust than the original model $\overline{v^2} - f$.

RESULTS AND DISCUSSION

Experiment setup

A propulsion characteristic experiment was carried out on the engine test cell under pure diesel mode of the marine DF engines. Test cell information was given in Table 1. When starting the engine, gradually adjusting the load and speed, adjusting the operating parameters of the engine oil, and cooling water system to the optimum value, the engine would be stabilized at 100% load operation (7800kW, 108r/min), measured in this condition to take the engine stability, the maximum explosion pressure, the compression end pressure, turbo speed, scavenging pressure, scavenging temperature, fuel consumption, emissions data, and so on. After taking calibration test conditions, gradually adjusting water and oil, and reducing engine power and speed, according to the propulsion characteristic, the engine would be stabilized successively at 75%, 50%, and 25% load (corresponding to speeds 96.1, 85.7, and 68 r/min) operation, measured engine operating data, and emissions under these conditions.

Table 1. Test cell information.

Analyzer	Model	Measurement ranges	Deviation
CO (10^{-6})	AIA-240	0~500	0.09%
CO_2 (%)	AIA-240	0~8	0.1%
NO (10^{-6})	FAC-246	0~2000	0.1%
O_2 (%)	IMA-241	0~25	0.1%
HC (10^{-6})	FAC-246	0~2000	0.08%
t (^{o}C)	T1308.3-022	0~600	1%
p (MPa)	T1308.3-013	0~5	1.6%
Speed (r/min)	FC-2010	0~3000	0.1%
Power (BHP)	CFSR-26	0~50000	0.25%

Calculation model

Modeling and meshing was by using AVL-FIRE software. The model and grid of marine DF engine combustion chamber were shown in Figure 1. The combustion chamber and fuel injector were of axis symmetrical structure, so the calculation region of the engine was taken as the original engine grid, the combustion chamber diameter was 500mm and the dynamic grid length was 2000mm. The technical specifications of the engine are given in Table 2.

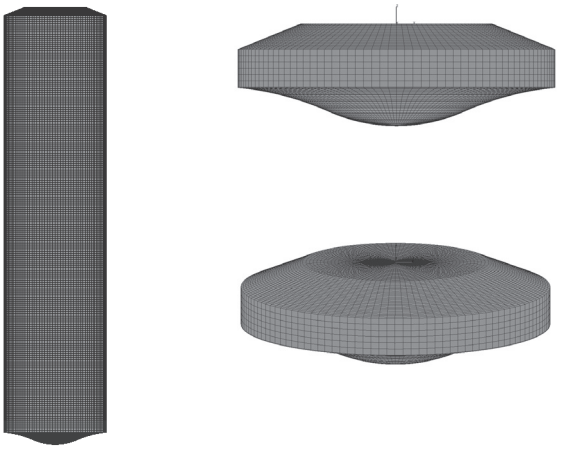

（a）222°CA （b）360°CA(TDC)

Figure 1. The model and grid of combustion.

In order to compare the differences of combustion progress by using different turbulence models for marine DF engine, the calculations assumed that the initial state of the cylinder pressure and temperature in cylinder was uniform. Throughout the calculation process, the cylinder is a closed system, and the heat transfer process was done according to a given wall temperature boundary conditions calculations. The calculation took into account the integral compression and power stroke, beginning with the scavenging port closed time (222 °CA) and ending with the exhaust valve open time (474 °CA); the top dead center was 360°CA.

Table 2. Technical specifications of the engine.

Item	Parameter
Bore (mm)	500
Stroke (mm)	2000
Rated rotate speed (r/min)	108
Rated power (kW)	7800
Fuel system type	Direct injection
Method of aspiration	Turbo-charging
Maximum cylinder pressure (MPa)	16.17
Charge air pressure (MPa)	0.387
Charge air temperature (K)	305
Coolant	water

Cylinder pressure analysis

The comparison of cylinder pressure between the experiment and three different turbulence models is shown in Figure 2. As shown in Figure 2, the cylinder pressure curves calculated by *k-ε* model, PANS model, and *k-ζ-f* model are very similar, with the difference having the greatest impact being in the fast combustion period. The cylinder pressure curve calculated by the *k-ε* model is the closest experimental values, the cylinder pressure curve calculated by the PANS

model is slightly higher than the experimental values, and the cylinder pressure curve calculated by the *k-ζ-f* model is slightly lower than the experimental values in the fast combustion period. The maximum explosion pressure calculated by the *k-ε* model is smaller 1.36% (0.22 MPa) than the experimental maximum explosion pressure; the maximum explosion pressure calculated by the PAN model is smaller 0.93% (0.15 MPa) than the experimental maximum explosion pressure; the maximum explosion pressure calculated by the *k-ζ-f* model is smaller 2.65% (0.43 MPa) than the experimental maximum explosion pressure. It can be seen in the three turbulence models. The *k-ε* model simulates the in-cylinder combustion process of the most accurate, but the exact, extent of the peak pressure, which is somewhat less than the PANS model.

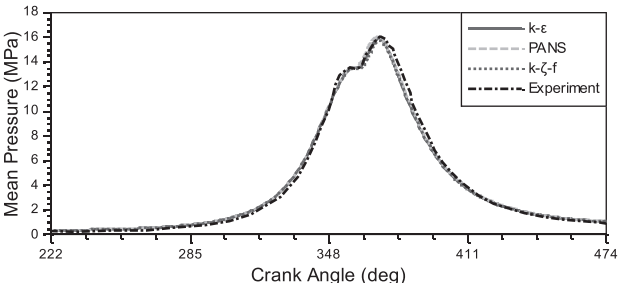

Figure 2. Comparison of mean pressure under different turbulence models.

Emissions analysis

Under three different turbulence models, the comparison of emission (O_2, NOx, CO_2 and CO) is illustrated in Figure 3 between the experimental value and simulation value.

As shown in (a), the O_2 emission curve calculated by *k-ε* model and *k-ζ-f* model is very approximate, but O_2 emission curve calculated by PANS model has big deviation from the experimental value, and the maximum deviation is about 2%.

As shown in (b), NOx emission curve calculated by *k-ε* model has the smallest deviation from the experimental value, but NOx emission curve calculated by PANS model is nearly two times larger than the experimental value, and NOx emission curve calculated by k-ζ-f model is larger than the experimental values by nearly 25%.

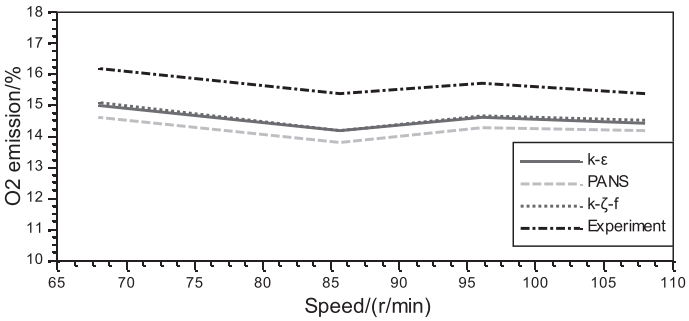

(a) O_2 emission

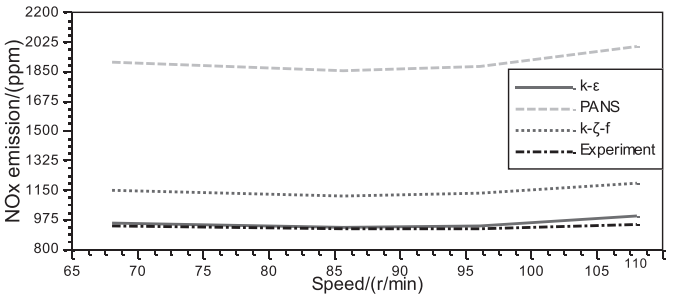

(b) NOx emission

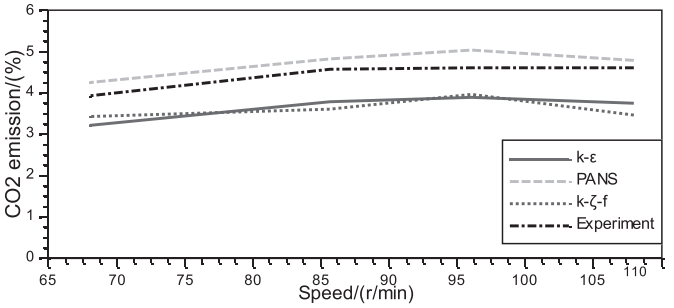

(c) CO_2 emission

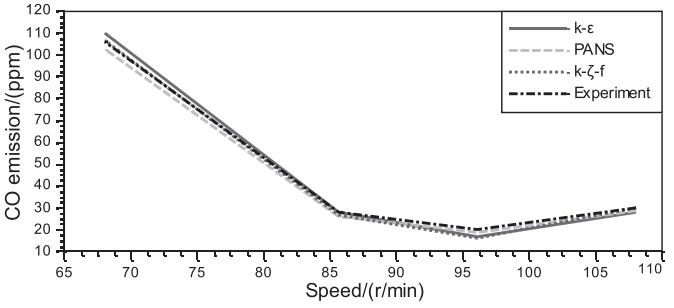

(d) CO emission

Figure 3. Comparison of emission under different turbulence models.

As shown in (c), CO2 emission curves calculated by k-ε model and k-ζ-f model are very approximate. CO2 emission curve calculated by PANS model is the minimum deviation from the experimental value, and the deviation is no more than 1%.The CO2 emission curve calculated by each turbulence model shows a "first close, then away, then close" variation with experimental values.

As shown in (d), as the load increases, CO emission calculated by k-ζ-f model is better agreement with experimental data when the engine is in a low load. However, when the engine is in the high load, CO emission calculated by PANS model is in better agreement with the experimental data.

CONCLUSION

The *k-ε* model is the most accurate to simulate the cylinder combustion process among the three turbulence models. The peak pressure in the cylinder is the largest by using PANS model and is in better agreement with the experimental data.

O2 emission and NOx emission curve calculated by PANS model have the maximum deviation from the experimental value, and the maximum deviation is about 2% and 1000 ppm, respectively.

As the load increases, CO emission curve calculated by turbulence model shows a "first close, then away, then close" variation with experimental values. When CO emission is calculated by the three turbulence models, k-ζ-f model is the most accurate in the low load, but PANS model is the most accurate in the high load.

ACKNOWLEDGMENT

This work was financially supported by the Scientific Research Projects from the Education Department of Liaoning Province (L201611).

REFERENCES

Abagnale C., Cameretti M.C., Simio L. De, Gambino M., Iannaccone S. & Tuccillo R. 2014. Numerical simulation and experimental test of dual fuel operated diesel engines. Applied Thermal Engineering **65**, 403-417.

Ai Yanting, Han Lei, Xu Xingyuan, Guo Xiaoling & Wang Zhi. 2015. Numerical investigation of thermal-acoustic-structural coupling in combustion chamber. Science Technology and Engineering **15**(5), 155-161.

Basara, B., Krajnovic, S. & Girimaji, S. 2010. PANS methodology applied to elliptic relaxation based eddy-viscosity transport model. Notes on Numerical Fluid Mechanics and Multidisciplinary Design **110**, 63-69.

Binbin Yang, Mingfa Yao, Wai K. Cheng,YuLi, Zunqing Zheng & Shanju L. 2014. Experimental and numerical study on different dual-fuel combustion modes fuelled with gasoline and diesel. Applied Energy **113**,722–733.

Brynolf, S., Fridell, E. & Andersson, K. 2014. Environmental assessment of marine fuels: liquefied natural gas, liquefied biogas, methanol and bio-methanol. Journal of Cleaner Production **74**, 86-95.

Chongmin Wu, Kangyao Deng & Zhen Wang. 2015. The effect of combustion chamber shape on cylinder flow and lean combustion process in a large bore spark-ignition CNG engine. Journal of the Energy Institute **1**, 1-8.

Debabrata Barik, Murugan S. 2014. Simultaneous reduction of NOx and smoke in a dual fuel DI diesel engine. Energy Conversion and Management **84**, 217-226.

Gan Tian, Wang Rugen, Zhang Jie & Li Shaowei. 2014. Numerical simulation of inlet distortion with interceptor with different turbulence models. Journal of Propulsion Technology **35**(7),891-896.

Girimaji, S. 2006. Partially-averaged navier-stokes model for turbulence: A reynolds-averaged navier-stokes to direct numerical simulation bridging method. Journal of Applied Mechanics **73**, 413-421.

Girimaji, S., Jeong, E. & Srinivasan, R. 2006. Partially-averaged navier-stokes model for turbulence: Fixed point analysis and comparison with unsteady partially-averaged navier-stokes. Journal of Applied Mechanics **73**, 422-429.

Han Chao, Zhang Pei, Ye Tao-hong & Chen Yi-liang. 2014. Large eddy simulation of CH4/air lifted flame. Journal of Propulsion Technology **35**(5), 654-660.

Henning Carlsson, Emil Nordström, Alexis Bohlin, Yajing Wu, Bo Zhou, Zhongshan Li, Marcus Aldén, Per-Erik Bengtsson & Xue-Song Bai. 2015. Numerical and experimental study of flame propagation and quenching of lean premixed turbulent low swirl flames at different Reynolds numbers. Combustion and Flame 162, 2582–2591.

Jin Ge, Zhang Zhixue & Gu Mingqi. 2008. Numerical simulation of QD128 aero-derivative gas turbine combustor. Aero engine **34**(2), 30-35.

José Antonio Vélez Godiño, Miguel Torres García, Fco José Jiménez-Espadafor Aguilar & Elisa Carvajal Trujillo. 2015. Numerical study of HCCI combustion fueled with diesel oil using a multizone model approach. Energy Conversion and Management **89**, 885–895.

Leiyong Jiang. 2012. A critical evaluation of turbulence modeling in a model combustor. ASME Turbo Expo **5**(3), 535-545.

Liu Chongyang & Dai Bin. 2014. Comparison and analysis of turbulent combustion models in numerical simulation of combustor, gas turbine experiment and research **27**(5), 12-18.

Mohand Said Lounici, Khaled Loubar, Lyes Tarabet, Mourad Balistrou, Dan-Catalin Niculescu & Mohand Tazerout. 2014. Towards improvement of natural gas-diesel dual fuel mode: an experimental investigation on performance and exhaust emissions. Energy **64**, 200-211.

Mongia H. C., Aviation GE. Cincinnati, & Ohio. 2008. Recent progress in comprehensive modeling of gas turbine combustion. AIAA Paper 2008-1445.

Sumit Roy, Ajoy Kumar Das, Rahul Banerjee & Probir Kumar Bose. 2014. A TMI based CNG dual-fuel approach to address the soot-NOx-BSFC trade-off characteristics of a CRDI assisted diesel engine-an EPA perspective. Journal of Natural Gas Science and Engineering **20**, 221-240.

Yee Chee See & Matthias Ihme. 2015. Large eddy simulation of a partially-premixed gas turbine model combustor. Proceedings of the Combustion Institute **35**,1225–1234.

Yu Hongliang, Duan Shulin & Sun Peiting. 2015. Effects of LNG gasification temperature on combustion and emission characteristics of marine dual fuel engines. Journal of Propulsion Technology **36**(9), 1369-1375.

Yu Hongliang, Duan Shulin & Sun Peiting. 2016. Effects of main/pilot timings on combustion and emission characteristics of marine dual fuel engines. Journal of Propulsion Technology **37**(9), 1735-1741.

Yuri P. Almeida, Paulo L.C. Lage & Luiz Fernando L.R. Silva. 2015. Large eddy simulation of a turbulent diffusion flame including thermal radiation heat transfer. Applied Thermal Engineering **81,** 412-425.

Zhou D.Z., Yang W.M., An H., Li J. & Shu C. 2015. A numerical study on RCCI engine fueled by biodiesel/methanol. Energy Conversion and Management **89,** 798–807.

Submitted: 16/11/2015
Revised : 12/11/2016
Accepted : 27/02/2017